

Article

Extraction of Urban Quality of Life Indicators Using Remote Sensing and Machine Learning: The Case of Al Ain City, United Arab Emirates (UAE)

Mohamed. M. Yagoub , Yacob T. Tesfaldet , Marwan G. Elmubarak and Naeema Al Hosani

Department of Geography and Urban Sustainability, UAE University,
Al Ain P.O. Box 15551, United Arab Emirates

* Correspondence: myagoub@uaeu.ac.ae



Citation: Yagoub, M.M.; Tesfaldet, Y.T.; Elmubarak, M.G.; Al Hosani, N. Extraction of Urban Quality of Life Indicators Using Remote Sensing and Machine Learning: The Case of Al Ain City, United Arab Emirates (UAE). *ISPRS Int. J. Geo-Inf.* **2022**, *11*, 458. <https://doi.org/10.3390/ijgi11090458>

Academic Editors: Samad Sepasgozar, Baojie He, Deo Prasad, Ali Cheshmehzangi, Wu Deng, Xiao Liu and Wolfgang Kainz

Received: 16 June 2022

Accepted: 17 August 2022

Published: 23 August 2022

Publisher's Note: MDPI stays neutral with regard to jurisdictional claims in published maps and institutional affiliations.



Copyright: © 2022 by the authors. Licensee MDPI, Basel, Switzerland. This article is an open access article distributed under the terms and conditions of the Creative Commons Attribution (CC BY) license (<https://creativecommons.org/licenses/by/4.0/>).

Abstract: Urban quality of life (UQoL) study is very important for many applications such as services distribution, urban planning, and socioeconomic analysis. The objective of this study is to create an urban quality of life index map for Al Ain city in the United Arab Emirates (UAE). The research aligns with the United Nations Sustainable Development Goals number ten (reduce inequalities) and eleven (sustainable cities and communities). In this study, remote sensing images and GIS vector datasets were used to extract biophysical and infrastructure facility indicators. The biophysical indicators are normalized difference vegetation index (NDVI), normalized difference water index (NDWI), modified normalized difference water index (MNDWI), soil adjusted vegetation index (SAVI), enhanced normalized difference impervious surfaces index (ENDISI), normalized difference built-up index (NDBI), land surface temperature (LST), slope, and land use land cover (LULC). In addition, infrastructure facility indicators such as distances to main roads, parks, schools, and hospitals were obtained. Additional infrastructure facility variables namely built-up to green area and build-up to bare soil area ratio were extracted from the LULC map. Machine learning was used to classify satellite images and generate LULC map. Random Forest (RF) was found as the best machine learning classifier for this study. The overall classification and Kappa hat accuracy was 95.3 and 0.92, respectively. Both biophysical and infrastructure facility indicators were integrated using principal component analysis (PCA). The PCA analysis identified four components that explain 75% of the variance among the indicators. The four factors were interpreted as the effect of LULC, infrastructure facility, ecological, and slope. Finally, the components were assigned weights based on the percentage of variance they explained and developed the UQoL map. Overall, the result showed that greenness has a greater effect on the spatial pattern of UQoL in Al Ain city. The study could be of a value to policy makers in urban planning and socioeconomic departments.

Keywords: urban quality of life; greenness; remote sensing; machine learning; principal component analysis (PCA)

1. Introduction

From the steam era till the present, the human way of living has changed dramatically [1]. The evidence of this rapid change is manifested by the growth of urban areas and the population living in cities. According to a United Nations [2] estimation, 68% of the world's population is expected to live in urban areas by 2050. However, rapid urbanization has many consequences collectively grouped as social and environmental problems. The social aspect comprises but is not limited to traffic congestion, crowdedness, racial disparities, and crime [3,4]. On the other hand, the environmental consequences of urbanization include but are not limited to, air pollution, water pollution, resource depletion, waste, and loss of green area [5,6]. In this context, the quality of urban life and sustainable urbanization has drawn the attention of researchers, politicians, and residents at large. Moreover, urban quality of life also outlined in the United Nations Sustainable Development Goal number

one (no poverty), two (zero hunger), ten (reduce inequalities), and eleven (sustainable cities and communities). In view of all that has been mentioned so far, the assessment of urban quality of life is indispensable to ensuring sustainable development within urban areas.

By definition, assessing the quality of urban life includes quantification of the relationship between the social and urban characteristics of a place in comparison to the perceived quality of life [7]. Urban quality of life can be explained using different aspects such as quantitative estimations, qualitative descriptions, perceptions, subjective wellbeing, and landscape features [8–10]. Furthermore, urban quality of life is the result of the interaction of various factors such as environmental, social, ecological, cultural, and so on. Due to the multi-dimensional nature of quality-of-life, there is no standard definition for urban quality of life [11,12]. Generally, researchers commonly use two approaches to assess the urban quality of life: objective and subjective approach [11]. In subjective approach people perception, attitude, and happiness are measured [13]. While in objective approach urban quality of life is assessed using indicators derived from observation, census, and satellite images [14]. For example, a study done by Tuan Seik [15] collected questionnaire from over 3000 people to estimate their overall life satisfaction. Some of the aspects of life measured are social life, family life, public services, environment, housing and health care. On the other hand, quality of life can be measured objectively by assessing the environmental and physical factors that could impact the livelihood of urban dwellers. For instance, environmental factors such as temperature, building density, greenness, accessibility to public services, and population density [16,17].

Urban quality of life is complex and has many dimensions, a single parameter analysis would not describe the complex nature of urban quality of life. Therefore, it is imperative to integrate more than one aspect of urban quality of life such as environmental, ecological, psychological, political, socioeconomic, and sociodemographic [18]. Field-based collections of quality-of-life indicators such as building density, green area, air quality, water availability, and surface temperature are very limited in space and has been a challenge. On the other hand, most of the socioeconomic and sociodemographic data are observed and collected directly from the site, which is costly and time consuming. Advances in remote sensing has improved the capability of remotely sensed images to be utilized for objective assessment of urban quality of life. As a result, urban quality of life assessment using remote sensing has received great attention. There are two main reasons for that: (1) remote sensing data with modest spatial resolution are publicly available and (2) the improvement in remote sensing image resolution and computation speed. Moreover, urban quality of life has different dimensions such as socioeconomic, spatial, and physical aspects. Hence, remote sensing provides superiority in providing the majority of the aspects of urban quality of life with spatially dense data [8]. Datasets derived from remote sensing are mainly grouped into two environmental indicators: biophysical and ecological. The biophysical indicators are, but are not limited to, normalized vegetation index (NDVI), normalized built-up index (NDBI), land surface temperature (LST), and land use land cover (LULC), while the ecological aspect includes aerosol optical depth [19–22]. Further processing of the data derived from remote sensing can be used to infer the socioeconomic aspect of urban life such as greening of the area, building density, and green area to building ratio. A study by Nichol and Wong [22] used remote sensing to produce a detailed map showing the urban quality of life in the Kowloon Peninsula, Hong Kong. Most importantly, the study found that relatively vegetation density explains most of the variability in urban quality of life. Similarly, a study done in Tehran indicated that remote sensing-derived parameters adequately captured the spatiotemporal variability of urban quality of life [11]. The finding is important because the urban quality of life is complicated and time-dependent that requires a holistic approach. Regardless of the climate and the extent of the study region, Nichol and Wong [23] showed that remote sensing-derived indicators are a reliable means of measuring the urban quality of life in tropical regions. Moreover, previous studies have shown that land use land cover can significantly affect ecosystem services and household

wealth [24,25]. Collectively, these studies outline a critical role of remote sensing-derived indicators in assessing quality of life in urban setting.

One major challenge is to integrate the indicators and generate urban quality of life index that is easily interpretable and signify their relative importance. Recent evidence suggests that there are two main approaches to integrate the indicators: weighted overlay and principal component analysis (PCA). In weighted overlay, each parameter is given arbitrary weight then the indicators are overlaid to produce quality of life index [26]. The main drawback of weighted overlay is the bias associated with giving weights for each indicator. On the other hand, PCA provides robust weighting criteria based on the percentage of variation explained by each component [7,8,27].

In this research, an objective assessment of urban quality of life from indicators derived from remote sensing was performed for Al Ain city. The objective approach is chosen because the indicators are easily accessible and spatially dense. Moreover, the quality-of-life indicators derived from remote sensing proved to provide satisfactory estimation of urban quality-of-life [7,28]. Although urban quality of life has been studied in different climatic zones, little attention has been paid to urban settings in arid environments. Moreover, with the advancement of cloud computation and different machine learning algorithms, satellite-derived urban quality of life indicators can be obtained with great accuracy. Urban life indicators such as build-up density and green area estimation depend on the classification accuracy of LULC images. Therefore, it is important to utilize models with the capability of classifying LULC with higher accuracy. Machine Learning (ML) is one of the models with the capability to take large data sets, structure them for relevance, mine them for insights, and ultimately create predictive/clustering capabilities based on models and algorithms [29]. ML has wide applications such as in text recognition, speech recognition, and image recognition [30,31]. ML was utilized in this study to classify the satellite images and produce land use land cover (LULC) Map. The LULC map was one of the components that were employed to determine urban quality of life (Section 3.3) and derive two indices (green to build-up ratio and building to bare soil ratio). In addition, the LULC data were correlated with urban quality of life indicators. Therefore, the LULC map is considered a crucial component in determining urban quality of life and the use of machine learning algorithm enhanced the classification accuracy.

There are two types of satellite image classification approaches: (a) traditional pixel-based image analysis and (b) object-based image analysis (OBIA). The OBIA classification has superiority on the counterpart pixel-based image analysis on the following aspects: it operates on similar pixels produced by image segmentation and more layers can be added to be used in classification; the object is composed of a group of pixels that has similar texture and shape; hence, object statistics can be computed and used to differentiate land cover classes with similar spectral signature [32]. In the same vein, Meneguzzo et al.'s [33] comparative study between OBIA and pixel-based image classification suggested that OBIA-based classification has better accuracy result [32,34,35]. For example, Nasir et al. [36] used object-based image analysis for LULC classification and change detection. The research found that OBIA has greater potential on classifying images derived from different sensors and resolution. Therefore, to implement LULC classification, OBIA-based supervised classification was chosen.

Furthermore, there are many ML algorithms (classifiers) such as minimum distance, random forest (RF), and support vector machines (SVM). The application of any algorithm depends on many factors such as data under study, spatial, and temporal characteristics. Hence, it is necessary to choose a classifier that suits the purpose of the analysis. Random forest (RF) classifier was used because previous studies showed its effectiveness in comparison to minimum distance and support vector machines (SVM). For example, Tokar et al. [37] used RF classification to classify Landsat 8 imagery and obtained classification accuracy of 80% within a reasonable speed. Moreover, utilization of RF and SVM for multiple identical datasets indicated that overall, RF classification has higher accuracy than the SVM algorithm [38].

The specific objective of this study was to investigate urban quality of life (UQoL) for Al Ain city from parameters derived from remotely sensed images and geographical information system (GIS). This study used the inductive approach where general quality of life in the city is determined based on specific indicators such as land use, infrastructure facility, land surface temperature, aerosol index, NDVI, and so on [11]. The authors familiarized themselves with the data, coded it, generated themes using classification, assigned names to the classes, and interpreted the classes (thematic analysis). To enhance the quality of indicators derived from remote sensing, object-based image classification using random forest classifier (RF) was implemented. The RF algorithm is an ensemble learning approach, where the classifier is made of a group of decision trees and each tree is produced from the training set. The RF algorithm is non-parametric and requires two parameters to set up the model [39]. Moreover, RF decision-making is simple to understand and the algorithm is robust for noise and outliers [40]. Furthermore, the present study integrates data derived from different satellites that include biophysical, ecological, and infrastructure facility variables to build a quality-of-life model. The results are expected to support urban sustainability efforts and provide more informed decisions for policymakers.

2. Material and Methods

2.1. Study Area

Al Ain city is located at $24^{\circ}03' \sim 24^{\circ}22' \text{ N}$ and $55^{\circ}28' \sim 55^{\circ}53' \text{ E}$, covering a total area of 765 square kilometer (km^2) and with an average elevation about 270 m above mean sea level. The city is located in the eastern region of the United Arab Emirates (UAE), and it is the fourth-largest and fastest-growing city in the UAE (Figure 1). The total population of Al Ain region is 770,000 and the population of Al Ain City is 284,730 [41]. The city has a hot desert climate with a mean annual temperature and rainfall of 36.5°C and 96.4 mm, respectively [42,43]. The presence of an oasis and low humidity weather makes it a popular destination for domestic and international tourists [44].

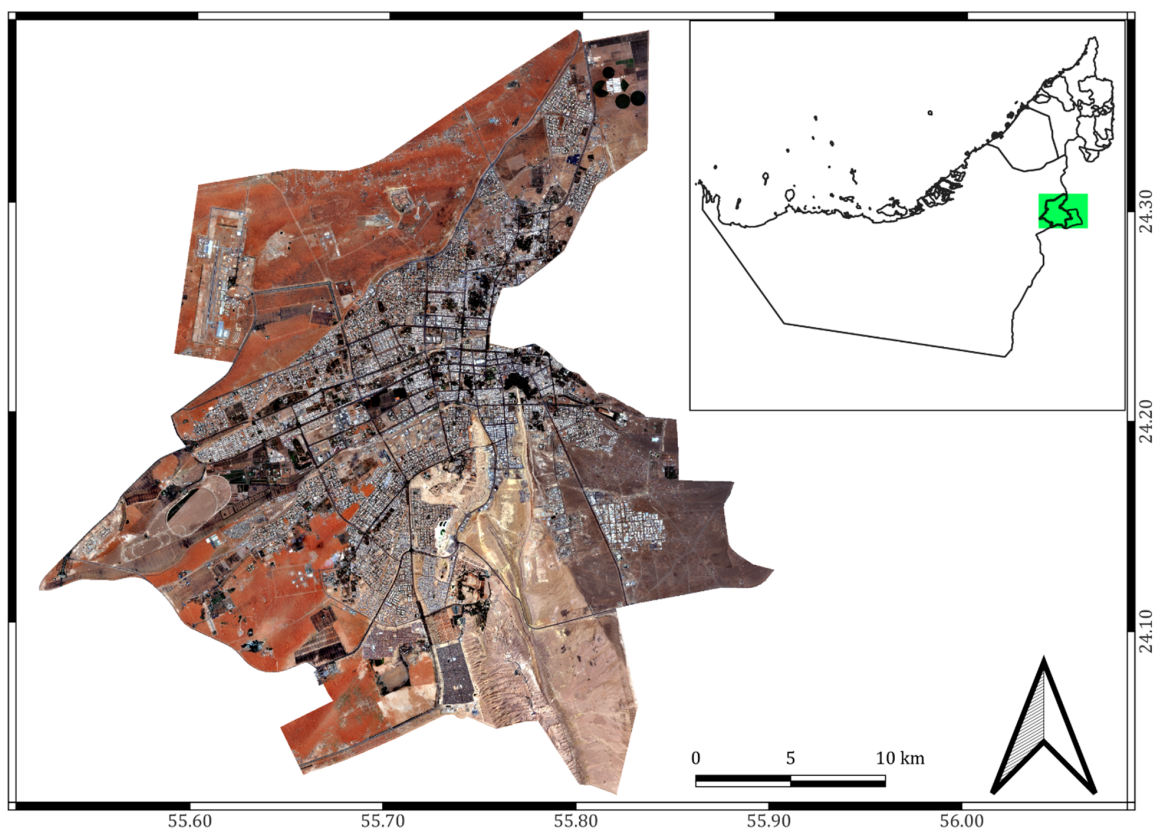


Figure 1. Location of the stud area: Al Ain Sentinel 2A image (left) and UAE map (right).

2.2. Datasets and Extraction of Environmental Variables

The present research utilized data from various sources: (1) Sentinel 2A and Sentinel 5P satellite images from August 2021, obtained from the European Space Agency (ESA) through GEE (Google Earth Engine); (2) Landsat TM satellite images from August 2021, obtained from the United States Geological Survey (USGS) through GEE; (3) Shuttle radar topography mission (SRTM) digital elevation from USGS; (4) GIS vector maps of Al Ain (hospitals, schools, parks, and roads) obtained from Al Ain Town Planning Department.

A total of 15 urban quality of life indicators are used from the above-mentioned sources to estimate UQoL (Table 1, Figure A2). The indicators are grouped into three categories: namely biophysical, ecological, and infrastructure facility indicators (Figure 2). The biophysical parameter derived from Sentinel 2A has 10 m spatial resolution, while the datasets derived from Landsat TM and SRTM have 30 m spatial resolution. The aerosol index derived from Sentinel 5P had 3.5 km × 5.5 km spatial resolution and resampled to 10 m spatial resolution.

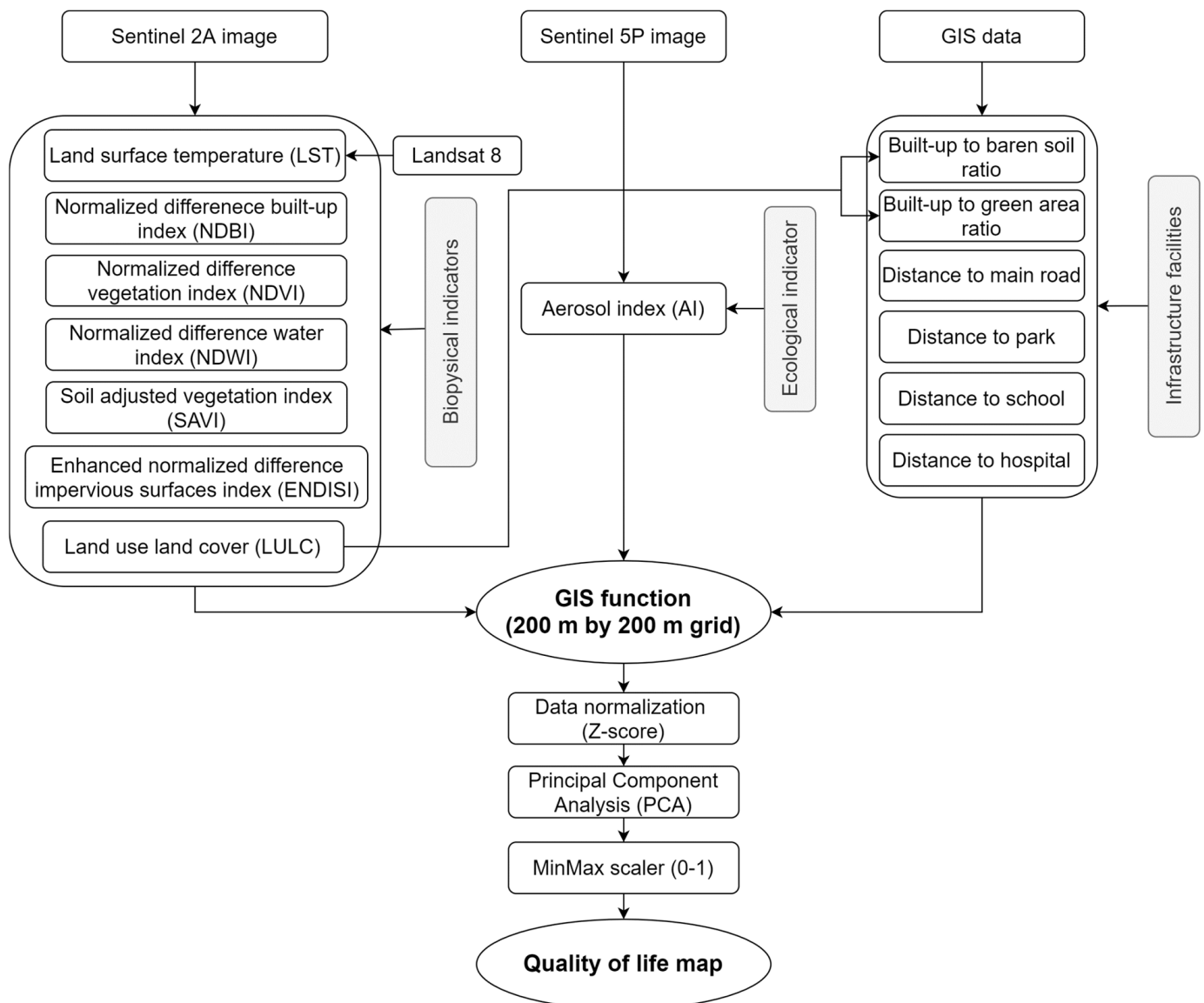


Figure 2. A flowchart of developing UQoL model for the study area.

The land surface temperature provides information on susceptibility of the area to urban heat island. Temperature is a useful indicator which depicts degree of comfort

and livability. Normalized difference build-up index was used to outline the impervious areas and buildings and it has an impact on variation of land surface temperature. While normalized difference vegetation index maps the green areas within the city. Green areas have positive relation with quality of life [45]. Normalized difference water index indicates the presence of water on the surface, which contributes positively to the perceived quality of life. Soil-adjusted vegetation index is similar to NDVI, and it is adjusted to correct the influence of soil brightness where the vegetation cover is low. Enhanced normalized difference impervious index has superiority over NDBI on separability of impervious surfaces [46]. The ecological indicator aerosol index was used to extract information related to the quality of air in the city. Furthermore, LULC map was generated to obtain green areas, baren soil area, and build-up areas. The infrastructure facility indicators namely road network, park location, school location, and hospital location were obtained in vector file. The distance to the nearest infrastructure facility indicator was calculated by measuring the shortest separation between them using distance to point and network analysis function in QGIS. In addition to this, other indirect infrastructure facility variables such as built-up to green area and built-up to bare land area were extracted from the LULC (Table 1).

Table 1. Urban quality of life indicators extracted from remote sensing and GIS vector data.

Indicator	Equation	No.	Reference	Format
AI *	$AI = 100 \times \log_{10} \left[\frac{R_{meas}(?2)}{R_{meas}(?1)} \right] - 100 \times \log_{10} \left[\frac{R_{calc}(?2, A_{LER}(?2))}{R_{calc}(?1, A_{LER}(?2))} \right]$	1	[47]	Raster
ENDISI *	$ENDISI = \frac{\rho_{Blue} - \beta \times \left(\frac{\rho_{SWIR1}}{\rho_{SWIR2}} + (MNDWI)^2 \right)}{\rho_{Blue} - \beta \times \left(\frac{\rho_{SWIR1}}{\rho_{SWIR2}} + (MNDWI)^2 \right)}$ $\beta = \frac{2 \times (\rho_{Blue})_{Mean}}{\left(\frac{\rho_{SWIR1}}{\rho_{SWIR2}} \right)_{Mean} + ((MNDWI)^2)_{Mean}}$	2	[46]	Raster
LST *	$LST = \frac{T_B}{1 + \left(\lambda \times \frac{T_B}{\rho} \right) \times \ln \epsilon}$	3	[48]	Raster
MNDWI *	$MNDWI = \frac{(Green - SWIR)}{Green + SWIR}$	4	[49]	Raster
NDBI *	$NDBI = \frac{(SWIR - NIR)}{(SWIR + NIR)}$	5	[50]	Raster
NDVI *	$NDVI = \frac{NIR - RED}{NIR + RED}$	6	[51]	Raster
NDWI *	$NDWI = \frac{NIR - SWIR}{NIR + SWIR}$	7	[52]	Raster
Slope *	$\tan \theta = \frac{rise}{run}$	8		Raster
SAVI *	$SAVI = \frac{(NIR - RED)}{(NIR + RED + L)} (1 + L)$	9	[53]	Raster
LULC *	OBIA-RF	10		Vector
Built-up to baren soil ratio *	$Ratio = \frac{Built_{area}}{Baren\ soil_{area}}$	11		Vector
Built-up to green area ratio *	$Ratio = \frac{Built_{area}}{Green_{area}}$	12		Vector
Distance to main road †				Vector
Distance to park †				Vector
Distance to school †				Vector
Distance of hospital †				Vector

* Data obtained from remote sensing; † Data obtained from GIS vector dataset.

2.3. Land Use Land Cover Classification Using a Machine Learning Algorithm

Land use land cover (LULC) map was prepared using supervised image classification. The steps followed include input data acquisition, preprocessing, classification, and accuracy assessment.

In input data acquisition, a cloud-free Sentinel-2A image along with supporting layers of digital elevation model (DEM) and NDVI was used. In preprocessing, a training and testing dataset was prepared to allow the algorithm to learn and validate the classification accuracy. The ratio between the training and testing dataset was set to 70:30, then the accuracy assessment was presented as a confusion matrix. The classification accuracy was checked with 700 random ground truth samples, and a confusion matrix was created.

The OBIA classification was performed following three processing steps: segmentation, class creation, and classification [54]. The first step is image segmentation and selecting optimum parameters for segmentation. A study conducted by Huang et al. [21] set segmentation parameter as: scale (20), shape factor (0.30), and compactness (0.5). However, the setting of the parameters has no unique solution and depends on many factors such as image characteristics, dataset size, and image resolution [55]. After a series of trial and error, the segmentation parameters for this study were set as follows: scale (50), shape factor (0.25), and compactness (0.5). The number of classes used for the classification are four (built-up, bare soil, green area, and highland). The last step is classification, which was done using RF classifier. Finally, the accuracy assessment was presented as a confusion matrix to validate the classification result. Following the preparation of the LULC, data on variables such as built-up to green area ratio and built-up to bare land were extracted.

2.4. Integration of Environmental and Infrastructure Facility Data

The first step in integration of urban quality of life indicators is to unify all data to a common grid cell size. There is no consensus on grid size resolution. For instance Sapena et al. [56] used a grid with resolution of 64 m × 64 m while Faisal and Shaker [57] used administrative divisions. There are many factors affecting the selection of the resolution such as purpose of the study, size of the study area, and speed of computer processing. In this study, a 200 m × 200 m resolution was found as an optimum resolution based on the mentioned factors. Therefore, environmental and infrastructure facility indicators were extracted from grid cells of 200 m spatial resolution. After extraction, the values of each parameter were normalized using Z-score by the Standard Scaler library in Python programming as follows:

$$Z = \frac{(x - u)}{\sigma} \quad (1)$$

where Z is the Z-score, x is the observed value, u is the mean of the sample, and σ is the standard deviation of the sample.

Following value normalization, all indicators were summarized using principal component analysis (PCA). Principal component analysis (PCA) has been applied by numerous researchers for UQoL analysis and was also used in this study [8,28,57]. The PCA is useful to retain the indicators that explain most of the variability among the considered variables. The PCA was computed using SPSS v.22 software and the suitability of the components for further computation were examined using Kaiser–Meyer–Olkin (KMO) and its significance test. The initial PCA components were rotated using the Varimax method to simplify the interpretation of the extracted factors and components with threshold eigenvalue greater than 1 were retained for UQoL analysis [58].

2.5. Urban Quality of Life Index and Validation Procedure

The urban quality of life index was computed following the method given by [45].

$$\text{UQoL} = \sum_1^n F_i W_i \quad (2)$$

where n is the number of factors selected, F_i factor i score, W_i the percentage of variance factor i . After the UQoL indicator for each grid was computed, the value was normalized between 0 and 1 using the MinMax scaler in Python programming. The data normalization simplifies the result for better interpretability and creates a map showing the spatial pattern of UQoL. The normalized UQoL were further classified into five classes following [59] suggestion: very poor (0.00 to 0.20), poor (0.21 to 0.40), moderate (0.41 to 0.60), good (0.61 to 0.80), and very good (0.81 to 1.00). The classified UQoL was mapped using QGIS to depict the spatial pattern of urban quality of life.

The effectiveness of the UQoL model was validated using regression analysis of representative indicator from the components. The original indicators with the highest loadings as an independent variable and the corresponding component score as a dependent variable. The indicators with highest loading were chosen because they have the highest influence within the component as suggested by Liang and Weng [8]. The accuracy of UQoL index depends on many factors such as remote sensing classification accuracy and GIS data accuracy. The classification accuracy was reported in the confusion matrix (Table 2) and the GIS database was checked for overshoot, undershoot, and sliver polygons. Sample of satellite images from each UQoL class (very poor, poor, moderate, good, and very good) were extracted from Google Earth and inspected visually to verify their agreement with the UQoL map.

Table 2. Confusion matrix.

Class Value	Built-Up	Bare Soil	Green Area	Highland	Total
Built-up	9099	1068	403	13	10,583
Bare soil	369	147,283	992	715	149,359
Green area	26	71	29,997	0	30,094
Highland	0	237	21	14,450	14,708
Total	9494	148,659	31,413	15,178	204,744
PA (%)	99.4	95.2	88.7	94.7	
UA (%)	86.0	98.6	99.7	98.2	
Kappa hat	0.82	0.97	0.99	0.98	
		Overall accuracy			95.3
		Kappa hat classification			0.92

3. Results

3.1. Land Use Land Cover Classification

The LULC for Al Ain city includes four main categories: built-up, bare soil, green area, and highland (Figure 3). The overall and Kappa hat accuracy of the classification was 95.3% and 0.92, respectively (Table 2). The LULC map shows majority of the built-up areas are concentrated in the central and southeast of the city. On the other hand, the outskirts of the city are surrounded by bare soil. The green areas are scattered throughout the city, and there are clusters of green areas at the tip of the northern part of the city that are related to farmland. The highland is categorized based on elevation and it is mainly clustered in the southern part of the city. From the LULC map, information about built-up to green area ratio, built-up to bare soil ratio, and the area of each land cover was extracted. The area of the city is mainly covered by bare soil (57%) followed by built-up (27%) and green area (11%).

3.2. Statistical Analysis

The descriptive statistics (mean, std, min, and max) of both biophysical and infrastructure facility variables are presented in Table 3. Relatively, the variability of AI (0.08 ± 0.13), SAVI (0.09 ± 0.07), NDWI (-0.05 ± 0.09), ENDISI (-0.13 ± 0.11), slope (4.95 ± 5.48), and LST ($43.16 \text{ }^\circ\text{C} \pm 13 \text{ }^\circ\text{C}$) indicator is higher among the biophysical parameters. In contrast, distance to school ($4080 \text{ m} \pm 3167 \text{ m}$) and distance to hospital ($8325 \text{ m} \pm 4561 \text{ m}$) has the highest variability among the infrastructure facility variables. The reason could be partially

explained by clustering of the schools and hospital in the eastern and southern side of the city.

Before running PCA analysis, all the indicators were subjected to Pearson correlation analysis. The correlation is essential for multivariate analysis and provides an overall relationship among the variables. Since the variables considered are many, only the important variables are presented here. A complete Pearson correlation analysis is provided in Appendix A: Figure A1.

Table 4 shows the relationship among the quality-of-life indicators and the area occupied by each LULC class. Generally, the correlation is low to moderate for most parameters. However, LST has strong positive relationship with bare soil area, while strong negative relationship with built-up areas. Since the city is located in desert, surface temperature expected to be high on bare soil than the built-up areas (Figure 4). Therefore, LST can be a useful variable for this study. The NDVI, SAVI, NDBI, and ENDISI have a strong relationship with built-up and green areas. Normalized difference vegetation index (Figure 4) and SAVI showed a very strong relationship ($r = 0.84$) with green area and negative relationship ($r = -0.09$, $r = -0.12$) with built-up area. On the other hand, NDBI and ENDISI showed strong negative relationship ($r = -0.73$, $r = -0.77$) with green area. Hence, both indicators can be invaluable variable for Al Ain quality of life study.

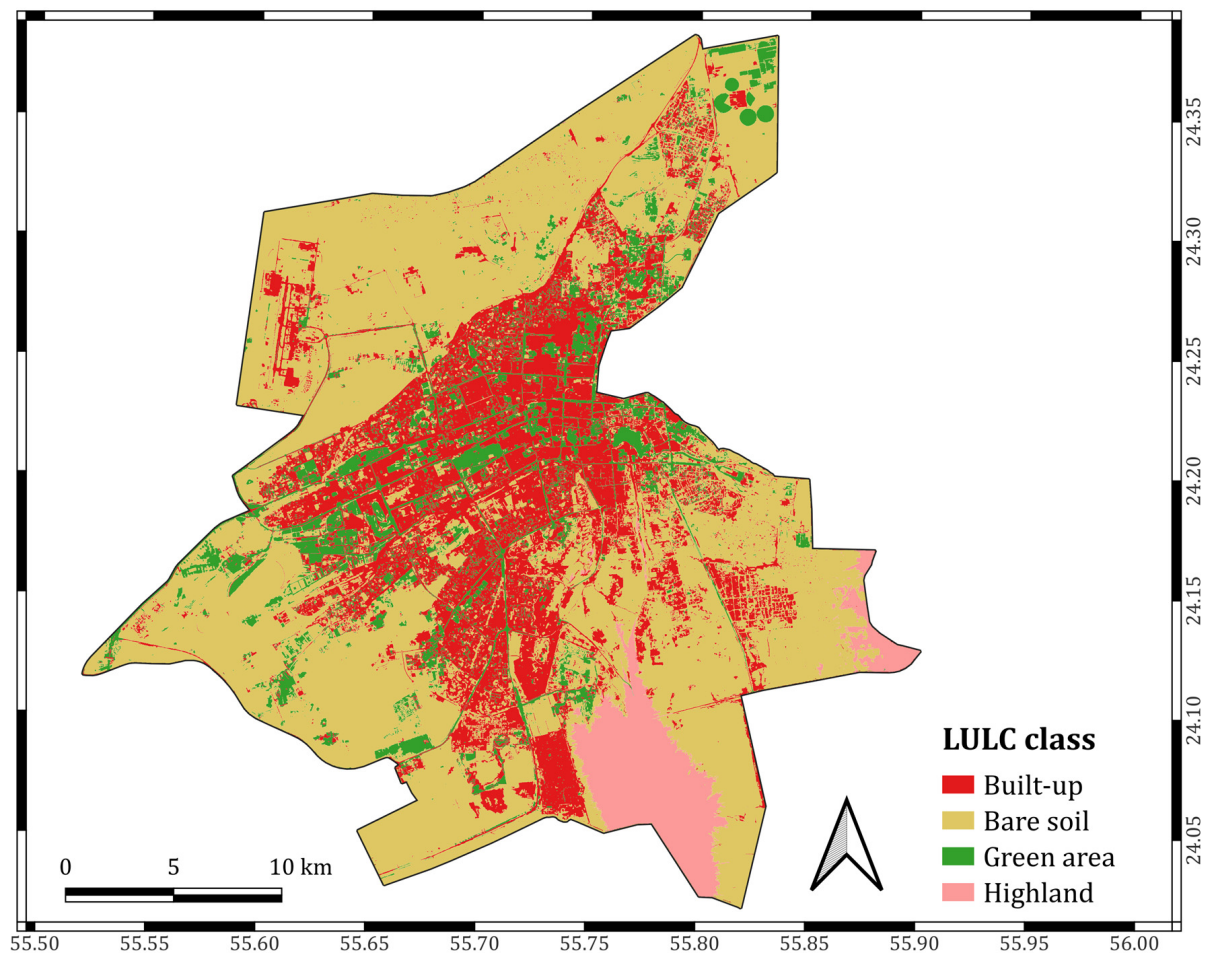


Figure 3. Land use land cover of map of Al Ain city.

Table 3. Descriptive statistics of biophysical and infrastructure facility indicators for Al Ain city.

	Mean	Std	Min	Max
AI	0.08	0.13	−0.16	0.36
SAVI	0.09	0.07	−0.20	0.68
NDWI	−0.05	0.09	−0.57	0.73
NDVI	0.10	0.07	−0.31	0.76
NDBI	0.10	0.08	−0.65	0.49
MNDWI	−0.33	0.09	−0.62	0.37
ENDISI	−0.13	0.13	−0.74	0.52
LST	43.16 °C	13 °C	31.37 °C	48.12 °C
Slope	4.95	5.48	0	68.86
Distance to school	4080 m	3167 m	0	15,134 m
Distance to road	1654 m	1835 m	0	10,191 m
Distance to park	4112 m	2769 m	0	14,270 m
Distance to hospital	8325 m	4561 m	0	21,340 m

Table 4. Correlation matrix between LULC areas and other environmental variables areas.

	Built-Up Area	Baren-Soil Area	Green Area	Highland Area
AI	0.37 ***	−0.41 ***	0.04 ***	0.23 ***
SAVI	−0.12 ***	−0.27 ***	0.84 ***	−0.09 ***
NDWI	0.42 ***	−0.66 ***	0.76 ***	−0.08 ***
NDVI	−0.09 ***	−0.29 ***	0.84 ***	−0.10 ***
NDBI	0.51 ***	0.65 ***	−0.73 ***	0.21 ***
MNDWI	0.77 ***	−0.63 ***	0.1 ***	−0.05 ***
ENDISI	0.02 *	0.28 ***	−0.77 ***	0.18 ***
LST	−0.38 ***	0.67 ***	−0.42 ***	−0.35 ***
Slope	−0.24 ***	−0.04 ***	−0.19 ***	0.6 ***
Distance to school	−0.5 ***	0.32 ***	−0.32 ***	0.36 ***
Distance to road	−0.37 ***	0.36 ***	−0.3 ***	0.08 ***
Distance to park	−0.44 ***	0.37 ***	−0.35 ***	0.20 ***
Distance to hospital	−0.46 ***	0.29 ***	−0.28 ***	0.33 ***

* $p < 0.05$; *** $p < 0.001$.

Principal component analysis was done for dimensionality reduction and get meaningful variables that explain majority of the variance in the dataset. The results of the principal component analysis with initial eigenvalues and after Varimax rotation are shown in Table 5. Based on the threshold eigenvalue greater than 1, four components were selected, and all together explains 75.3% of the variability of the input indicators. Overall, principal component 1 (PC1) represents the largest percentage of the variance of the data, with 26.26% of the total variance; the second component (PC2) 22.03%, the third component (PC3) 17.11%, and the fourth component (PC4) 9.90%. Hence, PC1 represents most of the biophysical indicators, including SAVI, NDWI, NDVI, NDBI, and ENDISI. The second factor is mainly concerned to infrastructure facility parameters, including distance to schools, roads, parks, and hospitals. The PC3 and PC4 represent ecological indicator and slope, respectively. Component loading is an important parameter to establish the magnitude and direction of relationship among the variables. PC1 has strong negative loading with three biophysical indicators: SAVI (−0.963), NDWI (−0.764), and NDVI (−0.969). On the contrary, PC1 has strong positive loading with two factors: NDBI (0.699) and ENDISI (0.828). This factor highlights adverse effect of land use; hence, the higher the score of this component, the lower the urban quality of life [59].

PC2 has strong positive loading with all infrastructure facility indicators: distance to school (0.92), distance to main roads (0.86), distance to parks (0.892), and distance to hospitals (0.753). Certainly, this factor has strongly linked to the public services and social equity. The higher the score of this component, the lower the urban quality of life. PC3 has strong positive loading with AI (0.838) and MNDWI (0.78), and strong negative loading with LST (−0.783). This component is related to ecological stress. Since higher slope

hinders services to goods and facilities, PC4 is concerned with the accessibility of the area. This component has strong positive loading with slope (0.862). The higher the score of this component, the lower the accessibility of the area.

The scores for each component with its spatial distribution are shown in Figure 5. As shown in Figure 5A, the majority of areas with the highest component score 1 (0.5–5.2) that is related to the effect of land use are on the outskirts of the city. Similarly, the highest value in the central part is related to built-up areas. In contrast, the lowest value of this component is in the central and northern parts of the city. The component score 2 that represents the infrastructure facility indicators is shown in Figure 5B. The figure clearly shows that the accessibility of public service is better in the central part of the city as opposed to the outskirts. This result may be explained by the fact that the central part is in proximity to public services such as main road, schools, hospitals, and parks. The pattern of component scores for ecological indicators is slightly different than the other components (Figure 5C). Ecologically, the best environment is in the southern part of the city, where NDWI is high and LST is low. The LST is low because the area is relatively at a higher elevation, where the highest Hafeet mountain is located. Figure 5D shows the component score for accessibility in the city. Generally, most of the city has a uniform score (−0.47 to 0.7) except in the southern part. Although the southern part is mountainous with lower LST and high NDWI, which is ideal for quality of life in desert environment, the accessibility to facility is low due to higher slope. Accordingly, the accessibility component score is very low (−1.86 to −8.15) for the southern part of the city.

Table 5. Rotated component matrix.

ID	Variables	Components and Loadings			
		1	2	3	4
1	AI	0.153	−0.093	0.838	0.034
2	SAVI	−0.963	−0.147	−0.019	0.108
3	NDWI	−0.764	−0.281	0.522	−0.199
4	NDVI	−0.969	−0.155	0.001	0.08
5	NDBI	0.699	0.349	−0.494	0.304
6	MNDWI	0.088	−0.228	0.78	−0.483
7	ENDISI	0.828	0.177	0.123	0.241
8	LST	0.398	0.107	−0.783	−0.321
9	Slope	0.145	0.053	0.094	0.862
10	Distance to school	0.147	0.92	−0.05	0.202
11	Distance to main road	0.132	0.86	−0.217	−0.178
12	Distance to park	0.182	0.892	−0.211	0.011
13	Distance to hospital	0.127	0.753	−0.034	0.335
14	Green to build-up ratio	−0.123	0.001	−0.01	0.004
15	Building to bare soil ratio	0.02	−0.04	0.084	−0.103
Initial eigenvalues		5.757	2.424	1.815	1.298
Eigenvalues after Varimax rotation		3.938	3.305	2.566	1.484
% Of variance		26.26	22.03	17.11	9.90
Cumulative variance		26.26	48.29	65.40	75.29
Weights calculated (%)		34.88	29.20	22.72	13.11

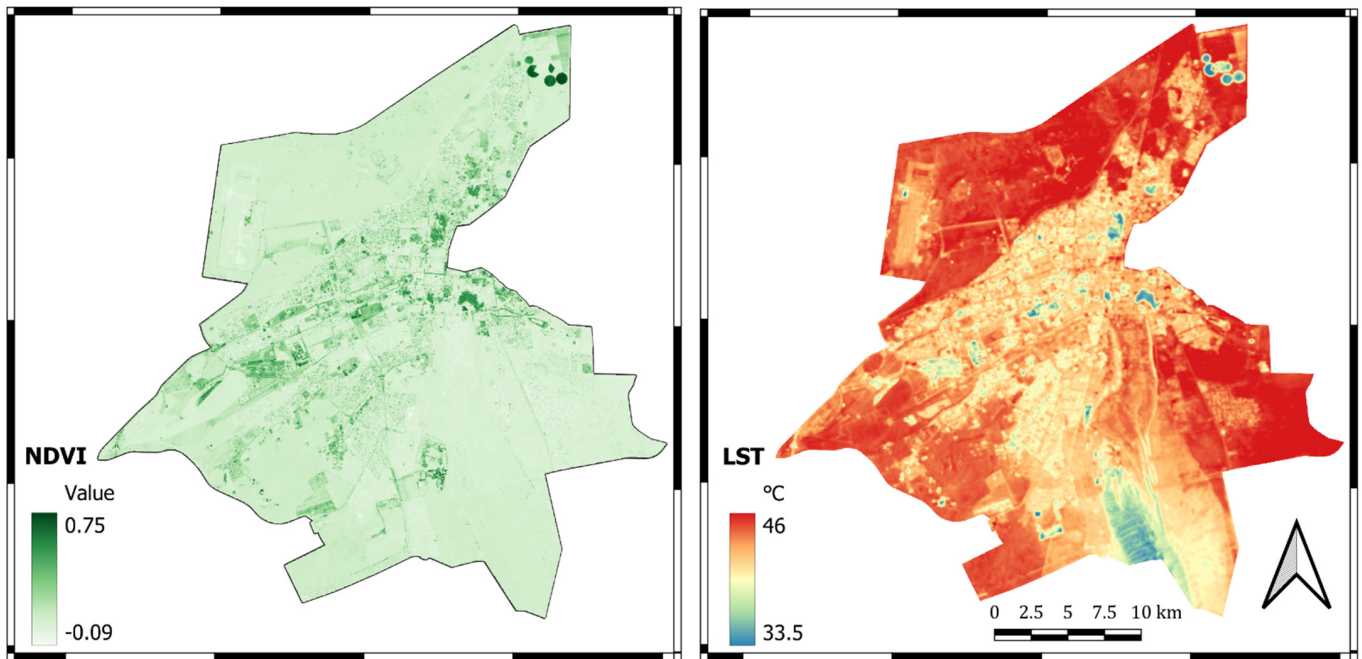


Figure 4. NDVI derived from Sentinel 2A (left) and LST derived from Landsat 8 image (right).

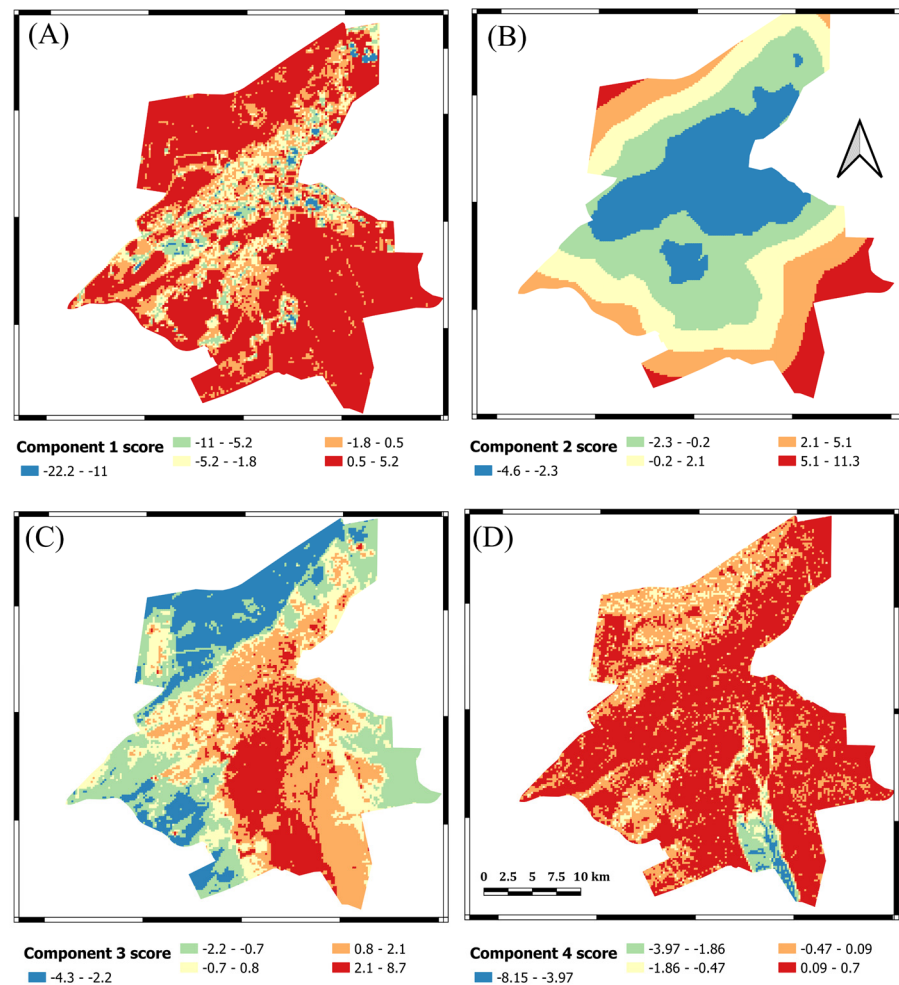


Figure 5. The four component scores: (A) effect of land use indicator, (B) infrastructure facility indicator, (C) ecological indicator, and (D) slope indicator.

3.3. Urban Quality of Life Index (UQoL)

The four-component score computed in Section 3.2 represent different aspects of urban quality of life. These are the effect of land use and greenness, infrastructure facility, ecological, and accessibility (slope). Therefore, all four components were combined to created UQoL map for Al Ain city (Figure 5). Since the increase in components 1, 2, and 4 are associated with poor quality of life, the scores were reversed by multiplying by -1 . Moreover, the component variance ratio was used as a weighting criterion for each component [28]. Finally, the UQoL was prepared as follows [8]:

$$\text{UQoL} = ((-34.88 \times \text{Component 1}) + (-29.20 \times \text{Component 2}) + (22.72 \times \text{Component 3}) + (-13.11 \times \text{Component 4})) \quad (3)$$

The spatial pattern of UQoL for Al Ain city is shown in Figure 6. Overall, the UQoL of Al Ain city is good. Since the city is located in desert, the uninhabited area of the city has poor to very poor UQoL. In contrast, the most inhabited area in the central part has moderate to very good UQoL. The reason is human settlement of the area are associated with the regreening activity and palm plantation. Moreover, public service accessibility and road network are better within the central part. However, even within the central part of the city there are areas with moderate to poor UQoL.

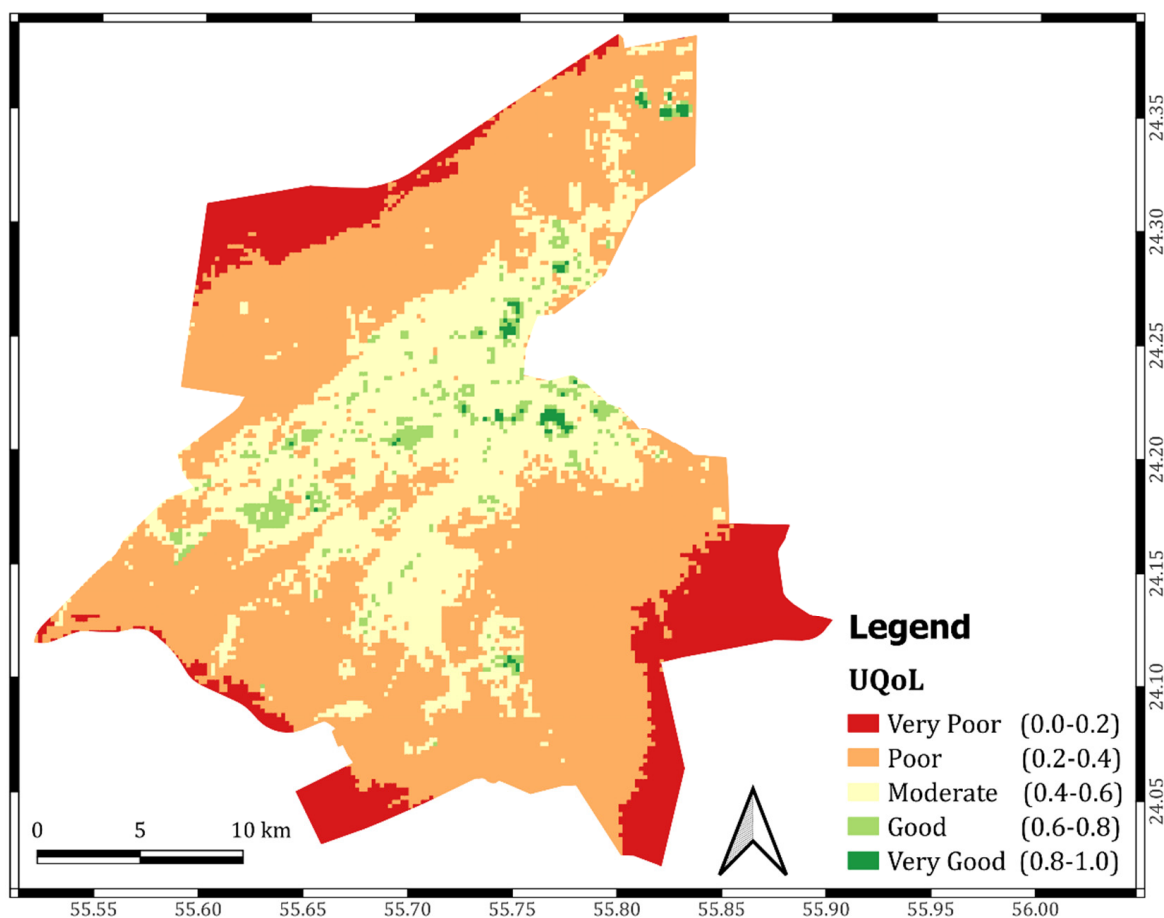


Figure 6. Urban quality of life index for Al Ain city.

Regression analysis is the most widely used validation method for UQoL index map. In this study, regression analysis of the three main components and visual inspection of sample class on Google Earth satellite image were performed to validate the result. The

environmental variables selected for regression analysis are the ones with the highest loading and variability within the study area. In the context of Al Ain city, PC1, PC2, and PC3 vary throughout the study area. On the other hand, PC4 is constant throughout the city except the southern part where the highland is located (Figure A2I). Therefore, PC1, PC2, and PC3 were selected to validate the UQoL index map. From PC1, PC2, and PC3, the dependent variables NDVI, distance to schools, and AI were selected, respectively. Overall, the R^2 is greater than 74%, indicating the model has explained majority of the variance in the UQoL (Table 6). Furthermore, visual inspection of the UQoL index map with Google Earth images suggests the model has performed well on outlining the spatial variability of quality of life. There are many parameters that could affect the variability within the city. However, the greenness factor has the highest influence, and areas with more green areas have a better UQoL index. For example, the outskirts of the city have the lowest index and almost no vegetation cover (poor to very poor). On the other hand, areas with a moderate index have sparse vegetation cover and moderate access to main road networks and public services. In contrast, good to very good index areas are located within the shortest distance to public services and the area is densely vegetated (Figure 7).

Table 6. Summary of the UQoL regression model.

Independent Variable	Dependent Variable	Loadings	R^2	Constant	Coefficient
Component 1 score	NDVI	−0.97	0.96 *	-2.91×10^{16}	−0.36
Component 2 score	Distance to school	0.92	0.89 *	4.07×10^{16}	0.31
Component 3 score	Aerosol index	0.84	0.74 *	1.57×10^{15}	0.44

* $p < 0.05$.

The result obtained could not be generalized because in many cities around the world, some high-income people live in the outskirts of the cities and the index could be good. Moreover, Al Ain city is surrounded by desert (The Empty Quarter) while other cities may be surrounded by farms (greenness) and the outskirts of the city may have better UQoL index. The contribution of the study is in crafting a methodology that utilized free available satellite images coupled with machine learning and statistical analysis to extract quality of life indicators and build empirical relationships. The approach could be used by other researchers especially in areas where there is a lack of socioeconomic data such as income, education, and health. There are some limitations with utilizing remote sensed derived data. These includes radiometric and geometric errors inherited in satellite images, low resolution of satellite images, errors related to algorithms (equations) used in image classification, calculation of indices, and generalization of LULC classes. Positional accuracy of vector data impact buffers around hospitals, parks, roads, and schools. Therefore, the result obtained provides a general guide about urban quality of life. Additional socio-economic data such as income and employment data (not available for the authors) could improve the result.

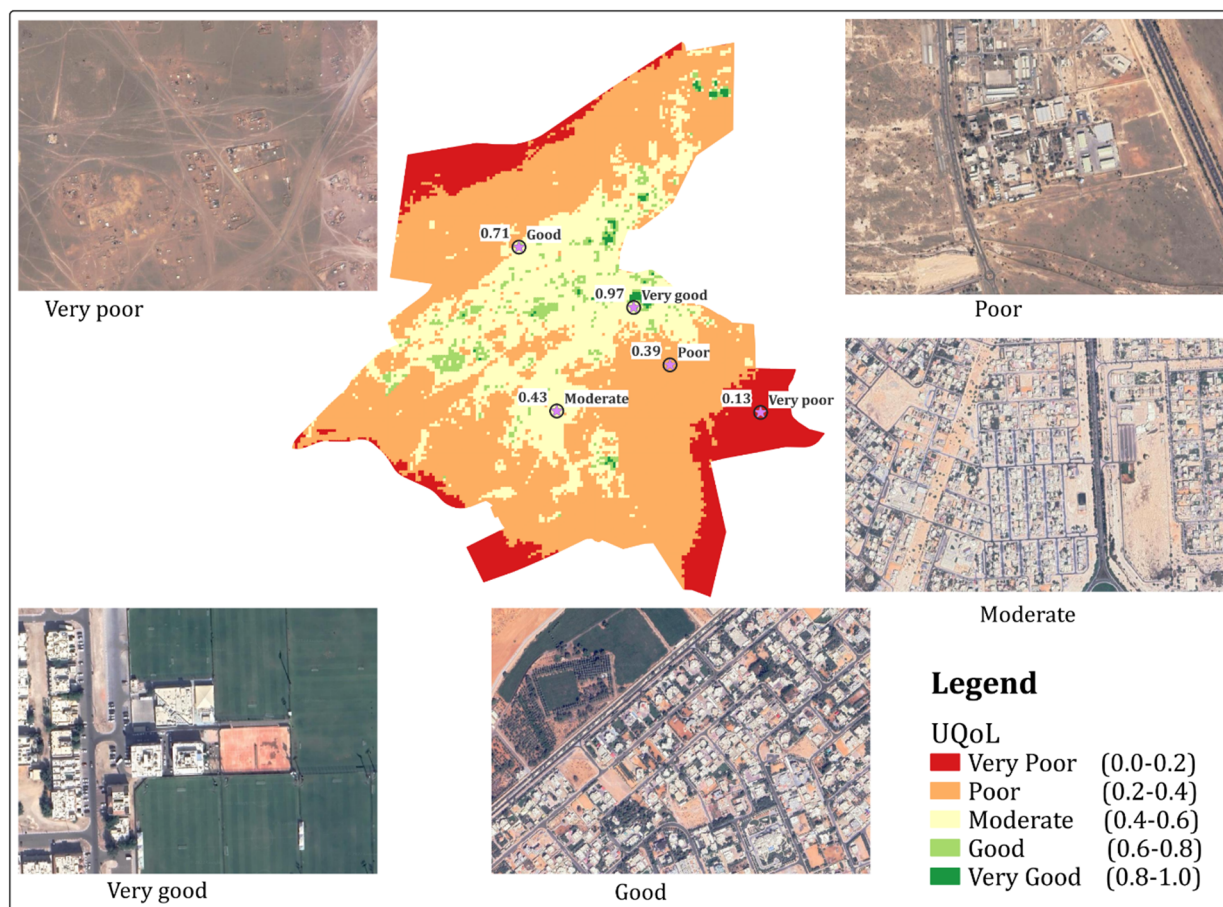


Figure 7. Visual inspection of UQoL index map.

4. Discussion

The UQoL study carried out in Al Ain city shows association between urban structure, environmental factors, and quality-of-life dimensions. Principal component analysis of all the variables used in the study indicates four components that explain 75.3% of the variability in UQoL. PC1 (biophysical indicators) has strong negative loading with SAVI (-0.963), NDWI (-0.764), and NDVI (-0.969). These variables indicate the urban greening and water availability. Greening and water availability provide various ecosystem service that indirectly improve human well-being. A subjective assessment of quality-of-life from a coastal desert megacity in Saudi Arabia found that urban green spaces have a positive impact on the well-being of urban dwellers [60]. The benefits are mental refreshment, physical activity, interaction with their children and relatives, and experience beauty of the nature.

In contrast, PC1 has strong positive loading with two factors: NDBI (0.699) and ENDISI (0.828). This factor highlights adverse effect of land use; hence, the higher the score of this component, the lowest the urban quality of life [59]. On the other hand, PC2 (infrastructure facility indicator) has strong positive loading with urban structure (distance to schools, roads, parks, and hospitals) indicating the importance of infrastructure on UQoL [20]. PC3 (ecological indicator) has strong positive loading with AI and MNDWI, while negative loading with LST. This component represents the effect of ecological indicators, and it has paramount relevance in the context of urban areas in desertic environment. Quality of life in desert environment is affected by the occurrence of dust storms, heat islands, and water shortage, which are sometimes referred as environmental factors [61]. PC4 has strong positive loading with slope indicating the accessibility of the area to different public

facilities. However, variability of slope within the study area is negligible. The exception is in the southern part of city (Highland area) where population density is very low (Figure 3).

Spatial variations of UQoL in Al Ain city is related to greening and human settlement. The reason is that the outskirts are covered by sand dunes, which have no human settlement or vegetation. Thus, the UQoL score for the areas with no dwellers is low (very poor to poor). In contrast, the highest UQoL scored areas are located in the central and northern parts of the city. Since the city is in the desert, the higher UQoL score among the inhabited areas indicates urban greening and/or socioeconomic factors. People with higher income tend to live in big houses with compound and garden, which positively affect the overall quality-of-life. A study done by Ma et al. [62] showed that quality of life has positive relationship with peoples level of income in both rural and urban setting. This result may be explained by the fact that green areas provide cooling effect, reduce exposure to air pollutants, and mental wellbeing [63]. The spatial variability of UQoL (poor to moderate) within the central part might be due disparity in income level which could affect the preference of large house with garden. These results further support the idea of urban quality of life has strong association with income levels of individuals [64]. In line with the present finding, a study conducted by Giannico et al. [65] found that the presence of green space positively predicts the overall perception of quality of life. On the contrary, there are few residential areas scored very low (very poor) located outside the central part of the city. The low score is due to inaccessibility to facilities and public services. In accordance with the present results, previous studies have demonstrated that improved public transport, easy access to facilities and services greatly improve urban quality-of-life [10].

Furthermore, the spatial pattern of high NDVI value and low LST value in Al Ain correlated well, which are important aspect of comfort in urban areas (Figure A1). The relationship indicates the cooling effect of vegetation, which attributes positively to urban quality life in desert environment. These results are in accordance with recent studies indicating that urban land cover controls spatial LST variation, which affects human quality of life [66]. A study done by Musse et al. [59] suggests, the income level of household greatly attributes to the spatial variability of urban quality-of-life. Furthermore, oasis expansion and desert sand stabilization greatly contribute to the greening of the desert [28]. All these factors add on to the improvement of quality of life in the desert environment. For this reason, the above-mentioned factors might attribute to the variability of UQoL within the inhabited area. From a visual inspection of the UQoL, vegetation cover variability can be noticed. Comparison of the findings with those of other studies confirms the importance of greening for improving UQoL [10,63,65]. The finding suggests that city planners need to focus on urban greening and urban infrastructure to improve the overall livelihood of the city residents.

5. Conclusions

Using traditional methods to assess quality of life in a city is time-consuming, costly, and inefficient. The improvement in remote sensing such as spatial resolution and development of new algorithms such as machine learning, and cloud computation has revolutionized extraction of quality-of-life indicators. In the present study, urban quality of life for Al Ain city was assessed using parameters derived from remote sensing and GIS vector data. The datasets derived from remote sensing are as follows: Sentinel 2A (NDVI, SAVI, NDWI, NDBI, ENDISI, MNDWI, and LULC), Sentinel 5P (AI), Landsat 8 (LST), and SRTM (slope). The GIS vector file contains infrastructure facility data, namely: distance to schools, roads, parks, and distance to hospitals. All parameters were normalized using Z-score before further analysis. Then the datasets from remote sensing and GIS vector data were integrated using PCA analysis and developed into a model to estimate the UQoL index. Based on PCA analysis, four components that have eigenvalue greater than 1 have accounted for 75% of the variability of the input datasets. In summary, the result of the present analysis showed that the UQoL of Al Ain city varies from moderate to very good in the central region. On the contrary, the outskirts of the city have the lowest index (poor

to very poor). There are many parameters that could affect the variability within the city. However, the greenness factor has the highest influence, and densely vegetated areas have a better UQoL index. The present finding can be used by urban planners, decision-makers, and charitable organizations to ensure the quality of life and sustainable development of urban areas. Further work is inevitable to establish and standardize the main factors that control urban-quality-of-life.

Author Contributions: Conceptualization, Mohamed. M. Yagoub and Yacob T. Tesfaldet; methodology, Yacob T. Tesfaldet and Mohamed. M. Yagoub; software, Yacob T. Tesfaldet; validation Mohamed. M. Yagoub and Yacob T. Tesfaldet, Marwan G. Elmubarak and Naeema Al Hosani; data curation Mohamed. M. Yagoub and Yacob T. Tesfaldet; writing—original draft preparation, Mohamed. M. Yagoub and Yacob T. Tesfaldet; writing—review and editing Mohamed. M. Yagoub, Yacob T. Tesfaldet, Marwan G. Elmubarak and Naeema Al Hosani; visualization, Yacob T. Tesfaldet; supervision, Mohamed. M. Yagoub; project administration, Mohamed. M. Yagoub; funding acquisition, Mohamed. M. Yagoub, Marwan G. Elmubarak and Naeema Al Hosani All authors have read and agreed to the published version of the manuscript.

Funding: This research was funded by United Arab Emirates University (UAEU) grant number [12H013] and the APC was funded by UAEU [12H013].

Institutional Review Board Statement: Not applicable.

Informed Consent Statement: Not applicable.

Data Availability Statement: The data used in this study is available from the corresponding author upon reasonable request.

Acknowledgments: Shehab Majud is acknowledged for his following up with the editing process. The invaluable suggestions and comments by the reviewers, and the following up by the editorial board of the ISPRS International Journal of Geo-Information are highly appreciated. The views and conclusions are those of the authors and should not be taken as those of the sponsor.

Conflicts of Interest: The authors declare no conflict of interest.

Appendix A

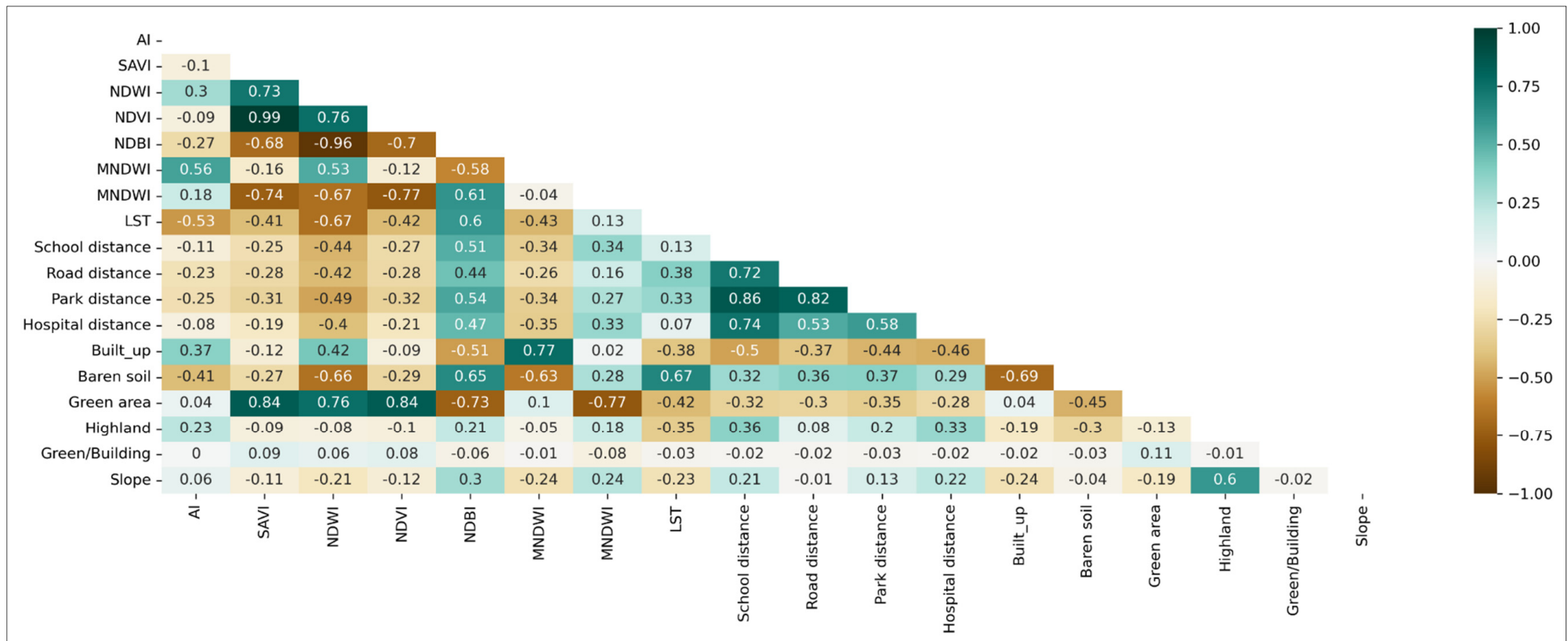


Figure A1. Correlation matrix among the environmental and infrastructure facility variables used for UQoL model.

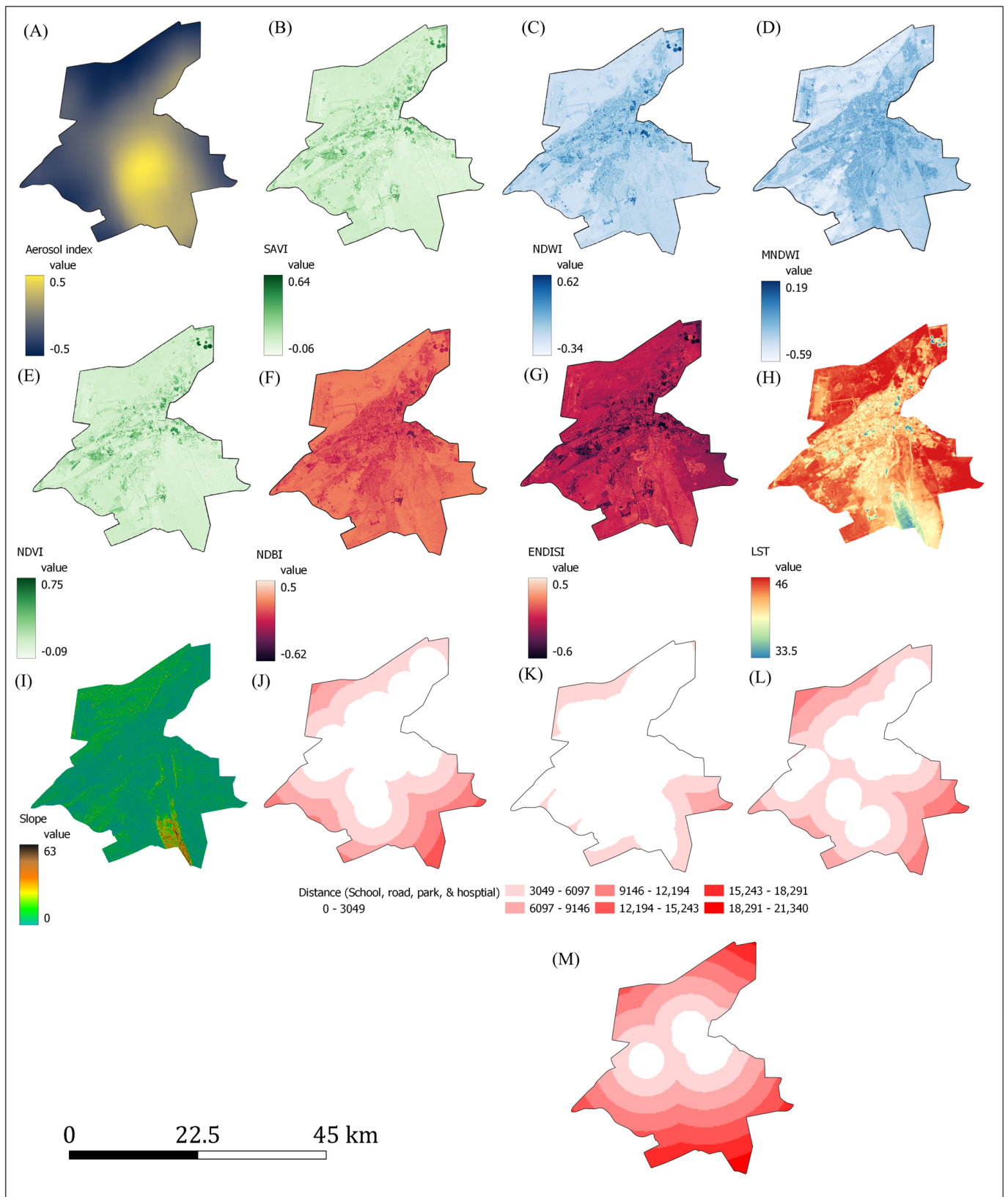


Figure A2. Urban quality of life indicators used for Al Ain city: (A) AI, (B) NDWI, (C) NDWI, (D) MNDWI, (E) NDVI, (F) NDBI, (G) ENDISI, (H) LST, (I) slope, (J) distance to school, (K) distance to main road, (L) distance to park, and (M) distance to school.

References

- Liang, W.; Yang, M. Urbanization, economic growth and environmental pollution: Evidence from China. *Sustain. Comput. Inform. Syst.* **2019**, *21*, 1–9. [CrossRef]
- United Nations. 68% of the World Population Projected to Live in Urban Areas by 2050, Says UN | UN DESA | United Nations Department of Economic and Social Affairs [WWW Document]. United Nations. URL. 2018. Available online: <https://www.un.org/development/desa/en/news/population/2018-revision-of-world-urbanization-prospects.html> (accessed on 1 July 2022).
- Britt, C.L. Social context and racial disparities in punishment decisions. *Justice Q.* **2000**, *17*, 707–732. [CrossRef]
- Soh, M.B.C. Crime and Urbanization: Revisited Malaysian Case. *Procedia—Soc. Behav. Sci.* **2012**, *42*, 291–299. [CrossRef]
- Liang, L.; Wang, Z.; Li, J. The effect of urbanization on environmental pollution in rapidly developing urban agglomerations. *J. Clean. Prod.* **2019**, *237*, 117649. [CrossRef]
- Zhang, X.; Han, L.; Wei, H.; Tan, X.; Zhou, W.; Li, W.; Qian, Y. Linking urbanization and air quality together: A review and a perspective on the future sustainable urban development. *J. Clean. Prod.* **2022**, *346*, 130988. [CrossRef]
- Merschdorf, H.; Hodgson, M.E.; Blaschke, T. Modeling Quality of Urban Life Using a Geospatial Approach. *Urban Sci.* **2020**, *4*, 5. [CrossRef]
- Liang, B.; Weng, Q. Assessing Urban Environmental Quality Change of Indianapolis, United States, by the Remote Sensing and GIS Integration. *IEEE J. Sel. Top. Appl. Earth Obs. Remote Sens.* **2011**, *4*, 43–55. [CrossRef]
- Macke, J.; Casagrande, R.M.; Sarate, J.A.R.; Silva, K.A. Smart city and quality of life: Citizens' perception in a Brazilian case study. *J. Clean. Prod.* **2018**, *182*, 717–726. [CrossRef]
- Mouratidis, K. Urban planning and quality of life: A review of pathways linking the built environment to subjective well-being. *Cities* **2021**, *115*, 103229. [CrossRef]
- Kazemzadeh-Zow, A.; Bolorani, A.D.; Samany, N.N.; Toomanian, A.; Pourahmad, A. Spatiotemporal modelling of urban quality of life (UQoL) using satellite images and GIS. *Int. J. Remote Sens.* **2018**, *39*, 6095–6116. [CrossRef]
- Bieda, A.; Telega, A. The Analysis of Research Hotspots in the Field of Urban Quality. *Sustainability* **2021**, *13*, 9582. [CrossRef]
- Pacione, M. Urban environmental quality and human wellbeing—A social geographical perspective. *Landsc. Urban Plan.* **2003**, *65*, 19–30. [CrossRef]
- Mostafa, A.M. Quality of Life Indicators in Value Urban Areas: Kasr Elnile Street in Cairo. *Procedia—Soc. Behav. Sci.* **2012**, *50*, 254–270. [CrossRef]
- Seik, F.T. Subjective assessment of urban quality of life in Singapore (1997–1998). *Habitat Int.* **2000**, *24*, 31–49. [CrossRef]
- Yadav, J.; Gupta, N. Urban Quality of Life: Domains, Dimensions and Indicators for Indian Cities. *IOP Conf. Ser. Earth Environ. Sci.* **2021**, *796*, 012032. [CrossRef]
- Chen, S.; Cerin, E.; Stimson, R.; Lai, P. An Objective Measure to Assessing Urban Quality of Life based on Land Use Characteristics. *Procedia Environ. Sci.* **2016**, *36*, 50–53. [CrossRef]
- Al-Qawasmī, J.; Saeed, M.; Asfour, O.S.; Aldosary, A.S. Assessing Urban Quality of Life: Developing the Criteria for Saudi Cities. *Front. Built Environ.* **2021**, *7*, 682391. [CrossRef]
- Behling, R.; Bochow, M.; Foerster, S.; Roessner, S.; Kaufmann, H. Automated GIS-based derivation of urban ecological indicators using hyperspectral remote sensing and height information. *Ecol. Indic.* **2015**, *48*, 218–234. [CrossRef]
- de Deus, L.R.; Garcia Fonseca, L.M.; de Marcelhas e Souza, I. Creating an socio-environmental condition index to assess of urban environmental quality. In Proceedings of the Joint Urban Remote Sensing Event 2013, Sao Paulo, Brazil, 21–23 April 2013; pp. 271–274. [CrossRef]
- Huang, H.; Li, Q.; Zhang, Y. A High-Resolution Remote-Sensing-Based Method for Urban Ecological Quality Evaluation. *Front. Environ. Sci.* **2022**, *10*, 765604. [CrossRef]
- Nichol, J.; Wong, M.S. Mapping urban environmental quality using satellite data and multiple parameters. *Environ. Plan. B Plan. Des.* **2009**, *36*, 170–185. [CrossRef]
- Nichol, J.; Wong, M.S. Modeling urban environmental quality in a tropical city. *Landsc. Urban Plan.* **2005**, *73*, 49–58. [CrossRef]
- Han, P.; Zhang, Q.; Zhao, Y.; Li, F.Y. High-resolution remote sensing data can predict household poverty in pastoral areas, Inner Mongolia, China. *Geogr. Sustain.* **2021**, *2*, 254–263. [CrossRef]
- Rahman, M.; Szabó, G. Impact of Land Use and Land Cover Changes on Urban Ecosystem Service Value in Dhaka, Bangladesh. *Land* **2021**, *10*, 793. [CrossRef]
- Rahman, A.; Kumar, Y.; Fazal, S.; Bhaskaran, S. Urbanization and Quality of Urban Environment Using Remote Sensing and GIS Techniques in East Delhi-India. *J. Geogr. Inf. Syst.* **2011**, *3*, 62–84. [CrossRef]
- Mackú, K.; Voženílek, V.; Pászto, V. Linking the quality of life index and the typology of European administrative units. *J. Int. Dev.* **2021**, *34*, 145–174. [CrossRef]
- Krishnan, V.S.; Firoz, C.M. Regional urban environmental quality assessment and spatial analysis. *J. Urban Manag.* **2020**, *9*, 191–204. [CrossRef]
- Wang, H.; Ma, C.; Zhou, L. A brief review of machine learning and its application. In Proceedings of the 2009 International Conference on Information Engineering and Computer Science, Wuhan, China, 19–20 December 2009. [CrossRef]
- Karita, S.; Watanabe, S.; Iwata, T.; Delcroix, M.; Ogawa, A.; Nakatani, T. Semi-supervised End-to-end Speech Recognition Using Text-to-speech and Autoencoders. In Proceedings of the ICASSP 2019 - 2019 IEEE International Conference on Acoustics, Speech and Signal Processing (ICASSP), Brighton, UK, 12–17 May 2019; pp. 6166–6170. [CrossRef]

31. Jamtsho, T.; Powdyel, K.; Powrel, R.K.; Bhujel, R.; Muramatsu, K. OCR and Speech Recognition System Using Machine Learning. In Proceedings of the 2021 Innovations in Power and Advanced Computing Technologies (i-PACT), Kuala Lumpur, Malaysia, 27–29 November 2021. [CrossRef]
32. Gao, Y.; Mas, J. A comparison of the performance of pixel based and object based classifications over images with various spatial resolutions. *Online J. Earth Sci.* **2008**, *2*, 27–35.
33. Meneguzzo, D.M.; Liknes, G.C.; Nelson, M.D. Mapping trees outside forests using high-resolution aerial imagery: A comparison of pixel- and object-based classification approaches. *Environ. Monit. Assess.* **2012**, *185*, 6261–6275. [CrossRef]
34. Balha, A.; Mallick, J.; Pandey, S.; Gupta, S.; Singh, C.K. A comparative analysis of different pixel and object-based classification algorithms using multi-source high spatial resolution satellite data for LULC mapping. *Earth Sci. Inform.* **2021**, *14*, 2231–2247. [CrossRef]
35. Tassi, A.; Gigante, D.; Modica, G.; Di Martino, L.; Vizzari, M. Pixel- vs. Object-Based Landsat 8 Data Classification in Google Earth Engine Using Random Forest: The Case Study of Maiella National Park. *Remote Sens.* **2021**, *13*, 2299. [CrossRef]
36. Nasir, S.M.; Kamran, K.V.; Blaschke, T.; Karimzadeh, S. Change of land use/land cover in kurdistan region of Iraq: A semi-automated object-based approach. *Remote Sens. Appl. Soc. Environ.* **2022**, *26*, 100713. [CrossRef]
37. Tokar, O.; Vovk, O.; Kolyasa, L.; Havryliuk, S.; Korol, M. Using the Random Forest Classification for Land Cover Interpretation of Landsat Images in the Prykarpattya Region of Ukraine. In Proceedings of the 2018 IEEE 13th International Scientific and Technical Conference on Computer Sciences and Information Technologies (CSIT), Lviv, Ukraine, 11–14 September 2018; pp. 241–244. [CrossRef]
38. Mansaray, L.R.; Wang, F.; Huang, J.; Yang, L.; Kanu, A.S. Accuracies of support vector machine and random forest in rice mapping with Sentinel-1A, Landsat-8 and Sentinel-2A datasets. *Geocarto Int.* **2019**, *35*, 1088–1108. [CrossRef]
39. Breiman, L. Random forests. *Mach. Learn.* **2001**, *45*, 5–32. [CrossRef]
40. Mountrakis, G.; Im, J.; Ogole, C. Support vector machines in remote sensing: A review. *ISPRS J. Photogramm. Remote Sens.* **2011**, *66*, 247–259. [CrossRef]
41. Statistics Centre. *Statistical Yearbook of Abu Dhabi 2020*; Statistics Center: Abu Dhabi, The United Arab Emirates, 2020.
42. Hejase, H.A.N.; Assi, A.H. Time-Series Regression Model for Prediction of Mean Daily Global Solar Radiation in Al-Ain, UAE, Time-series Regression Model for Prediction of Monthly and Daily Average Global Solar Radiation in Al Ain City—UAE. In Proceedings of the Global Conference on Global Warming 2011, Lisbon, Portugal, 11–14 July 2011.
43. Yagoub, M.M. Parks in Al Ain, UAE: Geographical Distribution, Opportunities, and Challenges. *Arab World Geogr.* **2014**, *17*, 24–41.
44. Yagoub, M.M.; Al Bizreh, A.A. Prediction of Land Cover Change Using Markov and Cellular Automata Models: Case of Al-Ain, UAE, 1992–2030. *J. Indian Soc. Remote Sens.* **2014**, *42*, 665–671. [CrossRef]
45. Li, G.; Weng, Q. Measuring the quality of life in city of Indianapolis by integration of remote sensing and census data. *Int. J. Remote Sens.* **2007**, *28*, 249–267. [CrossRef]
46. Chen, J.; Chen, S.; Yang, C.; He, L.; Hou, M.; Shi, T. A comparative study of impervious surface extraction using Sentinel-2 imagery. *Eur. J. Remote Sens.* **2020**, *53*, 274–292. [CrossRef]
47. ESA. Aerosol Index—Level-2 Processing—Sentinel-5P Technical Guide—Sentinel Online—Sentinel Online [WWW Document]. The European Space Agency. URL. 2022. Available online: <https://sentinels.copernicus.eu/web/sentinel/technical-guides/sentinel-5p/level-2/aerosol-index> (accessed on 27 May 2022).
48. Artis, D.A.; Carnahan, W.H. Survey of emissivity variability in thermography of urban areas. *Remote Sens. Environ.* **1982**, *12*, 313–329. [CrossRef]
49. Xu, H. Modification of normalised difference water index (NDWI) to enhance open water features in remotely sensed imagery. *Int. J. Remote Sens.* **2006**, *27*, 3025–3033. [CrossRef]
50. Zha, Y.; Gao, J.; Ni, S. Use of normalized difference built-up index in automatically mapping urban areas from TM imagery. *Int. J. Remote Sens.* **2003**, *24*, 583–594. [CrossRef]
51. Richards, J.A.; Jia, X. *Remote Sensing Digital Image Analysis, Remote Sensing Digital Image Analysis*; Springer: Berlin/Heidelberg, Germany, 1999. [CrossRef]
52. McFeeters, S.K. The use of the Normalized Difference Water Index (NDWI) in the delineation of open water features. *Int. J. Remote Sens.* **1996**, *17*, 1425–1432. [CrossRef]
53. Huete, A.R. A soil-adjusted vegetation index (SAVI). *Remote Sens. Environ.* **1988**, *25*, 295–309. [CrossRef]
54. Auquilla, A.; Heremans, S.; Vanegas, P.; Van Orshoven, J. A Procedure for Semi-automatic Segmentation in OBIA Based on the Maximization of a Comparison Index. In *Computational Science and Its Applications—ICCSA*; Springer: Cham, Switzerland, 2014; pp. 360–375. [CrossRef]
55. Hay, G.J.; Castilla, G. Geographic object-based image analysis (GEOBIA): A new name for a new discipline. In *Object-Based Image Analysis. Lecture Notes in Geoinformation and Cartography*; Blaschke, T., Lang, S., Hay, G.J., Eds.; Springer: Berlin/Heidelberg, Germany, 2008; pp. 75–89. [CrossRef]
56. Sapena, M.; Wurm, M.; Taubenböck, H.; Tuia, D.; Ruiz, L.A. Estimating quality of life dimensions from urban spatial pattern metrics. *Comput. Environ. Urban Syst.* **2020**, *85*, 101549. [CrossRef]
57. Faisal, K.; Shaker, A. An Investigation of GIS Overlay and PCA Techniques for Urban Environmental Quality Assessment: A Case Study in Toronto, Ontario, Canada. *Sustainability* **2017**, *9*, 380. [CrossRef]

58. Jolliffe, I.T. *Principal Component Analysis*, 2nd ed.; Springer-Verlag Inc.: New York, NY, USA, 2002.
59. Musse, M.A.; Barona, D.A.; Rodriguez, L.M.S. Urban environmental quality assessment using remote sensing and census data. *Int. J. Appl. Earth Obs. Geoinf.* **2018**, *71*, 95–108. [[CrossRef](#)]
60. Addas, A. Exploring the pattern of use and accessibility of urban green spaces: Evidence from a coastal desert megacity in Saudi Arabia. *Environ. Sci. Pollut. Res.* **2022**, *29*, 55757–55774. [[CrossRef](#)]
61. Khalil, H.A.E.E. Enhancing quality of life through strategic urban planning. *Sustain. Cities Soc.* **2012**, *5*, 77–86. [[CrossRef](#)]
62. Ma, L.; Liu, S.; Fang, F.; Che, X.; Chen, M. Evaluation of urban-rural difference and integration based on quality of life. *Sustain. Cities Soc.* **2019**, *54*, 101877. [[CrossRef](#)]
63. Markevych, I.; Schoierer, J.; Hartig, T.; Chudnovsky, A.; Hystad, P.; Dzhambov, A.M.; de Vries, S.; Triguero-Mas, M.; Brauer, M.; Nieuwenhuijsen, M.J.; et al. Exploring pathways linking greenspace to health: Theoretical and methodological guidance. *Environ. Res.* **2017**, *158*, 301–317. [[CrossRef](#)]
64. Thangiah, G.; Said, M.A.; Majid, H.A.; Reidpath, D.; Su, T.T. Income Inequality in Quality of Life among Rural Communities in Malaysia: A Case for Immediate Policy Consideration. *Int. J. Environ. Res. Public Health* **2020**, *17*, 8731. [[CrossRef](#)] [[PubMed](#)]
65. Giannico, V.; Spano, G.; Elia, M.; D'Este, M.; Sanesi, G.; Laforteza, R. Green spaces, quality of life, and citizen perception in European cities. *Environ. Res.* **2021**, *196*, 110922. [[CrossRef](#)] [[PubMed](#)]
66. Rahman, M.; Szabó, G. A Novel Composite Index to Measure Environmental Benefits in Urban Land Use Optimization Problems. *ISPRS Int. J. Geo-Inf.* **2022**, *11*, 220. [[CrossRef](#)]